Vol 14 No 10, October 2005
1009-1963/2005/14(10)/2019-07

Chinese Physics

© 2005 Chin. Phys. Soc.
and IOP Publishing Ltd

The propagation dynamics of ultraviolet light filament with Rayleigh scattering in air

Zhang Hua(张 华)†

Nantong University, School of Science, Nantong 226007, *China*

(Received 21 July 2004; revised manuscript received 30 May 2005)

In this paper we present for the first time the effects of Rayleigh scattering on the long distance propagation of ultraviolet (UV) light filament in air based on the stationary analysis. The simulation results show that the effects of Rayleigh scattering on the propagation of UV laser filaments may not be ignored. These influences are slightly dependent on the laser wavelength. We also compare the UV filament propagations at different input powers in the presence and the absence of the Rayleigh scattering and discuss the mechanisms of power loss and beam defocusing. In the absence of Rayleigh scattering, the filament propagation is determined by the oscillating behaviour of the beam size. In the presence of the scattering, the propagation lengths of filament are close to each other at different initial powers and determined by the Rayleigh scattering.

Keywords: filament, self-focusing, Rayleigh scattering
PACC: 4265J, 7385, 3380

1. Introduction

Since the first observation of infrared filaments in air by Braun *et al*[1] and Nibbering *et al*,[2] the generation of light filaments in air has become an active subject of experimental and theoretical research.[3−13] Light filaments are important not only due to the interest in their long distance propagation but also due to their other potential applications such as lighting protection[14−16] and lidar detection.[17,18] Numerous numerical attempts have been made to understand the propagation of infrared (IR) light filament according to a dynamical equilibrium.[5,19] The investigations of ultraviolet filament also have been reported at a wavelength of 248 nm in Refs.[7–10]

A general explanation for the formation of light filament, when its input power exceeds several times the critical power, is that during the initial stages of the propagation the beam is transversely focused into hot spots of high intensity under the combined actions of the optical Kerr effect and beam diffraction. The critical power is defined as the power at which self-focusing balances the beam diffraction. The self-focusing effect compresses the beam in the transverse diffraction plane, and the peak intensity increases correspondingly in the hot spots. The high intensities will produce nonlinear absorption via multi-photon ionization and electron plasma generation, along with plasma defocusing, which in turn restricts the growth of the hot spots and eventually causes their extinction. When the beam diffraction and plasma-induced defocusing balance the self-focusing, a stable self-guided light channel, referred to as the filament, is formed. Schwarz *et al* reported that this balance only resulted from the intensity-dependent mechanism in the case of UV filament.[7] Most researches have concentrated on the filaments around 800 nm. Since the peak intensities in these filaments exceed 100 TW/cm^2, and involve pulses with the duration being of the order of 100 fs or less, there appear many nonlinear effects and complex dynamic behaviours with them. But the peak intensity on axis is only 1 TW/cm^2, and the filaments can be created with the duration ranging from 500 fs to 1ns in the UV (248 nm). As a consequence, most of the higher order nonlinear effects that are important in the near-IR can be neglected. For that reason longer pulses should travel longer distance since more energy can be trapped in the filaments. One should be able to obtain the long propagation distances by increasing the duration of the UV laser beam. Schwarz *et al* also derived an analytical solution of ultraviolet filaments

†E-mail: zh@ntu.edu.cn

for long pulses (in the order of nanoseconds) based on the stationary analysis.[8] They neglected the effects of Rayleigh scattering on the propagation of UV filaments at 248 nm.

The purpose of the present study is to present the propagation dynamics of the long pulse UV filaments including the Rayleigh scattering and demonstrate the effects of Rayleigh scattering on the UV filament propagation. First, we determine the interested pulse duration scales in which the theory is applied. Then we present the numerical solutions of the UV filaments and investigate the effect of Rayleigh scattering in the long distance propagation. Finally, we compare the UV filament propagations at different input powers and discuss the mechanisms of power losses and beam defocusing.

2. The interested pulse duration scale

The upper limit of the pulse duration to form the filaments is set by the inverse bremsstrahlung. Due to a light filament, the electron plasma existing in an intense field will gain energy through the inverse bremsstrahlung.[20] If the energy of electrons is equal to the ionization potential of neutral molecules, the electrons will impact on and then ionize neutral molecules, allowing the electron density to grow rapidly in a cascade ionization process. The multiphoton ionization is not dominant in this case. Thus the delicate balance between self-focusing and plasma defocusing that sustains the filaments will be destroyed. The energy gain $\mathrm{d}E$ of the electrons due to the inverse bremsstrahlung in the time interval $\mathrm{d}t$ follows[20]

$$\mathrm{d}E = \frac{2Ie^2\nu_{\mathrm{ei}}}{\varepsilon_0 c m_{\mathrm{e}}\omega^2}\mathrm{d}t, \tag{1}$$

where I is the beam intensity, ω the laser frequency, m_{e} the electron mass, and ν_{ei} the electron–ion collision frequency. The time interval Δt in which the electron energy reaches the ionization potential W_{i} through the inverse bremsstrahlung is

$$\Delta t = \frac{\varepsilon_0 c m_{\mathrm{e}}\omega^2}{2Ie^2\nu_{\mathrm{ei}}}W_{\mathrm{i}}. \tag{2}$$

We define Δt as the upper limit of the pulse duration. The ionization potential of oxygen is 12.2 eV. The electron–ion collision frequency ν_{ei} is determined by the following equation:[17]

$$\nu_{\mathrm{ei}} = \frac{3\times10^{-6}N_{\mathrm{e}}\ln\Lambda}{T_{\mathrm{e}}^{1.5}}, \tag{3}$$

where N_{e} is the electron density in units of cm^{-3} and T_{e} is the electron temperature in units of eV which is defined roughly as the excess energy of an electron after the ionization. For example, the photon energy at 248 nm is 5eV. T_{e} equals 2.8eV for three-photon ionization of oxygen. $\ln\Lambda$ is the Coulomb integral which is in the range $1 \le \ln\Lambda \le 10$ and taken as 5 in our case.

Here we are to estimate the upper limit Δt. The beam intensity on axis is $1.3\times10^{12}\mathrm{W/cm}^2$ for a Gaussian beam with an input power of 345MW and initial beam waist of 130μm. We choose three UV wavelengths of 248, 266 and 290 nm, which can be supplied by an excimer amplifier system,[7] a frequency-quadrupled Nd:YAG laser and a Ce:LiCAF crystal amplifier,[21] respectively. The longest pulse durations in which the UV filaments can form are 4.3 ns, 2.1 ns and 0.4 ns at the wavelengths of 248, 266 and 290 nm, respectively. Therefore, this limit for the UV filament is about three orders of magnitude larger than that for the IR filament since the IR intensity is about 100 times larger and the frequency is triple lower. This means that only UV nanosecond pulses can be used to produce the long distance filament propagation.

One can pursue the stationary solution of the filament propagation in the case of long pulses. The lower limit of the pulse duration used for the stationary analysis of UV filament is determined by the response time of the electron plasma. In the approximation that the number of electrons remains small compared to the number of neutrals (for example, the density of oxygen N_0=$5.4\times10^{18}\mathrm{cm}^{-3}$ at sea level) and that the number of positive ions is equal to the number of electrons, the rate equation for the generation of electrons is obtained as follows:[8]

$$\frac{\mathrm{d}N_{\mathrm{e}}}{\mathrm{d}t} = \sigma^{(3)}I^3N_0 - \beta_{\mathrm{ep}}N_{\mathrm{e}}^2, \tag{4}$$

where N_{e} is the electron density, I the beam intensity, $\sigma^{(3)}$ the three-photon ionization coefficient of oxygen and $\sigma^{(3)}$=$7.36\times10^{-29}\mathrm{cm}^6\mathrm{s}^2/\mathrm{J}^3$, β_{ep} is the electron–ion recombination coefficient which is a function of the electron temperature and $\beta_{\mathrm{ep}} = 1.138\times10^{-11}T_{\mathrm{e}}^{-0.70}$.[15] Considering that the number of oxygen molecules is about 21% in air, one obtains β_{ep} =$1.2\times10^{-12}\mathrm{m}^3/\mathrm{s}$ at 248 nm. The effects of electron attachment have been neglected in Eq.(4).[8] We also ignore the avalanche ionization because here we seek for the lower limit of the pulse duration.

Assuming that the temporal light pulse is approximated by a step function for simplicity, we obtain the

electron density as a function of pulse rising time during the pulse propagation by solving Eq.(4). The numerical results show that the electron density reaches 75% of its equilibrium density in 30, 25 and 17ps for the wavelengths of 248, 266 and 290 nm, respectively. We conclude that lower limits of pulse duration are 30, 25 and 17ps. One can apply the stationary analysis to UV pulses of duration ranging from a few tens of picoseconds to several nanoseconds.

It should be demonstrated that the interested pulse duration scales applying to the stationary analysis are related to the beam power. We also investigate the dependence of the interested time scales on the beam power. The upper and lower limits of the pulse duration are shown in Fig.1 for different input powers. As expected, initially the upper and lower limits both decrease quickly as the power increases because the frequency of collision between free electrons and surrounding air molecules increases.

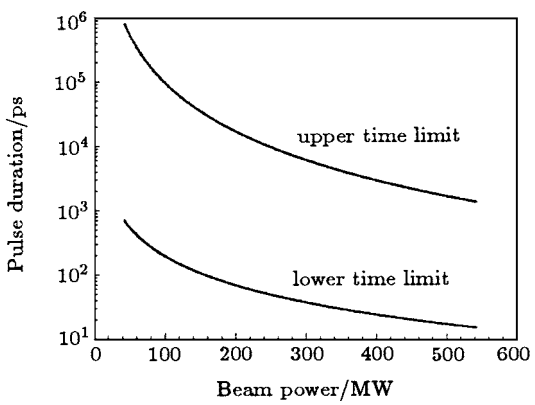


Fig.1. The interested time scale of the pulse duration versus the beam power, in which the steady-state analysis is applied to the UV filament in air.

3. Evolution of the pulse power and beam size

The propagation of intense light pulses is governed by the Maxwell's equations:

$$\left[\Delta_{\text{transv}} + \frac{\partial^2}{\partial z^2} - \frac{n_0^2}{c^2}\frac{\partial^2}{\partial t^2}\right]\mathcal{E}\,\mathrm{e}^{\mathrm{i}(wt-kz)} = \mu\frac{\partial^2 P_{\text{NL}}}{\partial t^2}, \tag{5}$$

where $\mathcal{E}$ is the envelop of the light pulses. The linear properties of the medium polarization have been incorporated in the index n_0 as follows:

$$P_{\text{NL}} = \left(\varepsilon_0\chi^{(3)}\left|\mathcal{E}\right|^2 + \varepsilon_0\chi^{(4)}\left|\mathcal{E}\right|^3\right)\mathcal{E}\,\mathrm{e}^{\mathrm{i}(wt-kz)}. \tag{6}$$

For the propagation of long pulses being of the order of nanosecond in duration, we consider it as a stationary problem and neglect the time term in Eq.(5), and have

$$\left[\Delta_{\text{transv}} - 2\mathrm{i}k\frac{\partial}{\partial z}\right]\mathcal{E} = -\frac{\omega^2}{c^2}\left[\chi^{(3)}\left|\mathcal{E}\right|^2 + \chi^{(4)}\left|\mathcal{E}\right|^3\right]\mathcal{E}. \tag{7}$$

Assuming that the beam profile is approximately a Gaussian profile, we have

$$\mathcal{E}(r,z) = \frac{w_0}{w(z)}\varepsilon_0\mathrm{e}^{-r^2/w(z)^2}\mathrm{e}^{-\mathrm{i}(kr^2/2R(z)-\Psi(z))}. \tag{8}$$

Substituting Eq.(8) into Eq.(7) and applying the stationary analysis model,[8] one obtains a differential equation describing the evolution of the beam size:

$$\frac{\mathrm{d}^2 w}{\mathrm{d}z^2} = -\frac{4P}{k^2P_{cr}}\frac{1}{w^3} + \frac{4}{k^2}\frac{1}{w^3} + \frac{6\ell}{n_0}\beta_4 P^{3/2}\frac{1}{w^4}, \tag{9}$$

where P is the beam power, w the beam size, P_{cr} the critical power, $\beta_4 = -(2/\pi)^{3/2}\bar{n}_3/\ell$ is the plasma absorption coefficient, $\bar{n}_3$ is the plasma nonlinear refraction index, $\ell = c/2\nu_{\text{ei}}$ is the free path of the electrons in the plasma. The first term on the right-hand side of Eq.(9) describes the self-focusing, the second is diffraction and the third is plasma defocusing.

Considering the power loss through the 3-photon ionization, plasma absorption and Rayleigh scattering, one obtains the complete expression of the nonlinear attenuation of the beam power,[8]

$$\frac{\mathrm{d}P}{\mathrm{d}z} = -\beta_3\frac{1}{w^4}P^3 - n_0\beta_4\frac{1}{w^3}P^{5/2} - \alpha_{\text{R}}P, \tag{10}$$

where $\beta_3 = 3\hbar\omega\sigma^{(3)}N_0(2/\pi)^2$ is the power attenuation coefficient associated with the 3-photon ionization. α_{R} is the Rayleigh scatter coefficient. The first term on the right-hand side of Eq.(10) is the power attenuation through the photon ionization, the second is the plasma absorption and the third is the power loss through the Rayleigh scattering. One finds the Rayleigh scattering at 248 nm corresponds to a power attenuation coefficient of $\alpha_{\text{R}}=5\times10^{-4}\text{m}^{-1}$. Thus the filament propagation associated with 3-photon ionization of the oxygen including the Rayleigh scattering in air is described completely by Eqs.(9) and (10).

4. Propagation dynamics of the UV filament with regard to Rayleigh scattering

We solve numerically Eqs.(9) and (10) to obtain the pulse power and beam size during the filament

propagation. To demonstrate the effect of Rayleigh scattering, we have plotted the beam size, beam power and electron density over a distance of 2 km for an input power of 58MW and an initial beam waist of 130μm. Figure 2 shows the filament sizes without the Rayleigh scattering (solid line) and with Rayleigh scattering (dashed line) at a wavelength of 248 nm. It can be seen that the filament can propagate more than 2km when the Rayleigh scattering is neglected. But the filament defocuses at a distance of about 500 m in the case of the scattering. The Rayleigh scattering reduces significantly the propagation distance of UV filament. But there is no significant difference over the first 100 m, the beam sizes stay confined below 200μm. In this regime the power loss is dominated by the 3-photon ionization of oxygen and hence the effect of Rayleigh scattering can be neglected. Figure 3 shows the electron density in the filament. Over the first 100 m, there appears no obvious difference in electron density between the presence and absence of the Rayleigh scattering. After the filament propagates about 300 m the electron density decrease by one order of magnitude and scattering loss becomes more and more pronounced. In order to understand the power loss, we plot the beam power as a function of the propagation distance in Fig.4. In the case of Rayleigh scattering, after about 500 m the beam power decreases down to 34 MW, which is very close to the critical power (31 MW). The beam loses too much power to be trapped and the filament is diffracted because of the photon ionization and Rayleigh scattering.

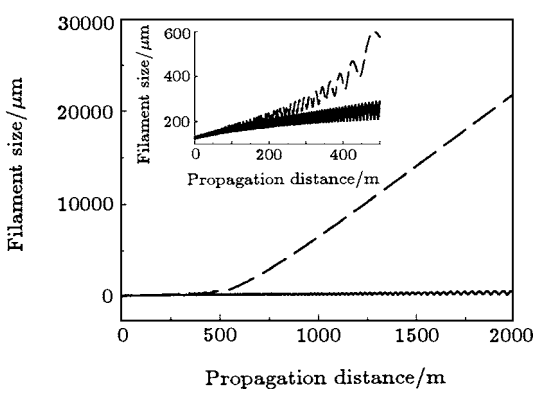


Fig.2. Propagation dynamics of a 58 MW filament over 2 km. The solid line shows the behaviour without the Rayleigh scattering, the dashed line denotes the behaviour with the Rayleigh scattering. The inset depicts the propagation of the filament over the first 500 m.

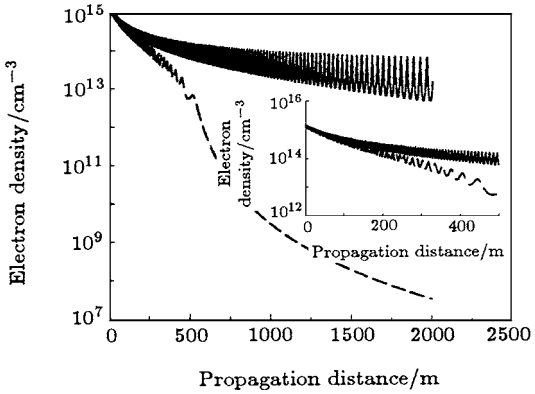


Fig.3. Electron density of a 58 MW filament over the first 2 km. The solid line shows the behaviour without the Rayleigh scattering, the dashed line denotes the behaviour with the Rayleigh scattering. The inset depicts the propagation of the filament over the first 500 m.

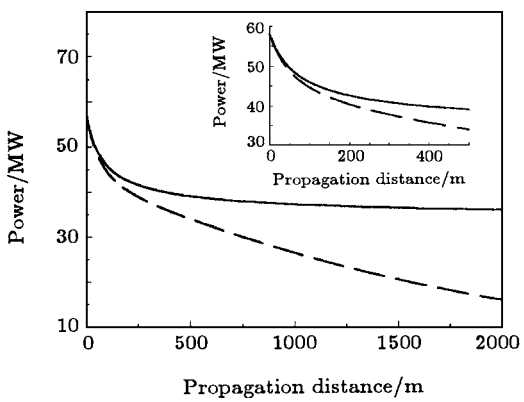


Fig.4. Beam power of a 58 filament over the first 2 km. The solid line is for the behaviour in the absence of the Rayleigh scattering, the dashed line is for the behaviour in the presence of the Rayleigh scattering. The inset depicts the beam power over the first 500 m.

In the case of no scattering, the filament can still continue to propagate over 2 km although the beam power decreases down to 40 MW in the first 500 m. The power lost along the travelling distance seems to be lower than the expected. The explanation for this unexpected low loss is sought to be due to the size oscillation of the beam. To understand this point, the electron density (dashed line) and the beam size (solid line) are plotted in Fig.5 as a function of the distance ranging from 450 m to 500 m. As the beam size decreases down to 235μm, the electron density sharply peaks at above 10^{14}cm^{-3}; as the beam further expands it falls and returns to an insignificant value. The beam waist appears to "ricochet" in every period at a minimum value. In most cases, the power loss is high only in a small fraction of period where the beam size is small. The loss decreases with distance because

that fraction of period spent in the beam of the shortest dimension decreases with distance (see Fig.3) as the oscillation period increases. This phenomenon is the steady state analogue of "dynamic replenishment" observed in the numerical simulation by Mlejnek *et al.*[19]

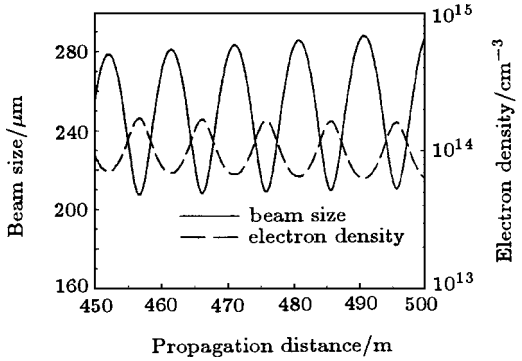


Fig.5. Beam size (solid line) and electron density (dashed line) in the distances ranging from 450 m to 500 m. The significant ionization only occurs over the short lengths in which the beam confinement is maximal.

We also compare such effects at different wavelengths. Rayleigh scatter coefficient α_R is greatly dependent on the wavelength: $\alpha_R \propto 1/\lambda^4$. The Rayleigh scattering coefficients are estimated to be $3.7\times10^{-4}\mathrm{m}^{-1}$ and $2.6\times10^{-4}\mathrm{m}^{-1}$ respectively for 266 nm and 290 nm. Figure 6 shows the beam sizes as a function of propagation distances at different wavelengths for an input power of 58 MW over the first 1000 m. It can be seen that the behaviours of the beam sizes in the filaments are similar for the three wavelengths over the first 500 m. The filaments of 248 nm defocus at a distance of 500 m but the filaments of 266 nm and 290 nm defocus at distances of about 600 m and 700 m, respectively. The propagation distances of filaments for the three wavelengths are close to each other approximately. So the effects of Rayleigh scattering on the filament propagation for the three wavelengths all cannot be neglected.

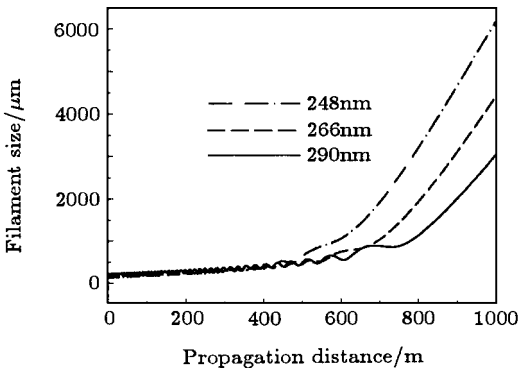


Fig.6. Comparison of filament propagations at different wavelengths for an input power of 58 MW.

5. The comparison of various input powers

The propagation dynamics of a 58 MW input power beam has been investigated above. In this section the behaviours for four different input powers are studied, namely 58 MW, 100 MW, 185 MW and 345 MW. The behaviours of 58 and 185 MW beams are of particularly interest because they mark the crossing points of minimum and maximum beam sizes,[8] at which the minimum and maximum beam sizes of oscillation are equal at the beginning of propagation. The beam sizes in the filaments are plotted as a function of distance in Fig.7 with and without regard to the Rayleigh scattering loss for input powers of 58, 100, 185 and 345 MW. One can find two features from Fig.7. The first feature is that a higher input power is not necessarily beneficial to a long distance propagation when the Rayleigh scattering is disregarded; the second one is that the propagation distances of filaments for the four input powers are very close to each other when the Rayleigh scattering is included.

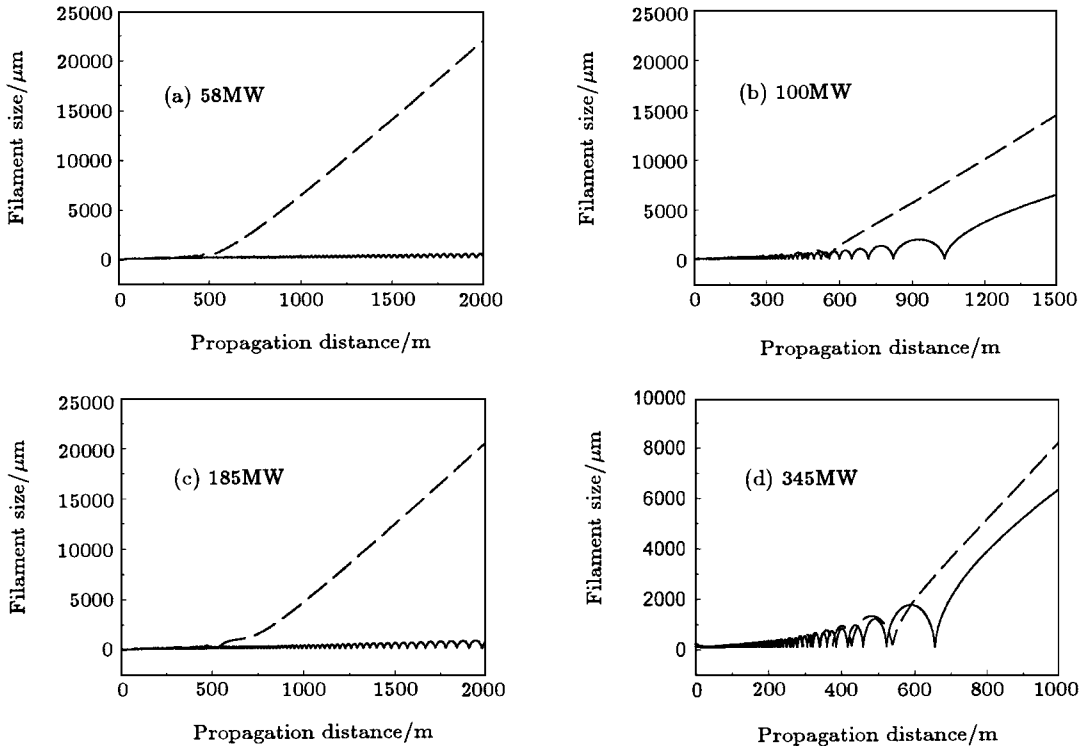


Fig.7. Comparison of filament sizes versus the distance for input powers of 58, 100, 185 and 345 MW. The solid lines are for the behaviour without the Rayleigh scattering, the dashed lines are for the cases including Rayleigh scattering.

In order to understand the first feature, we plot the power in the filament as a function of distance in Fig.8. It can be seen that most of the initial power is consumed in the first 100 m at either a higher input power or lower input power. After an initial decay over 100 m, the filament power remains at a constant level between 45 and 55 MW. The reason is that the larger input power can cause more electron plasma. To illustrate that point we define the electron number per unit meter as

$$N_{\mathrm{em}} = \frac{\pi}{2} w^2 N_{\mathrm{e}}. \tag{11}$$

The electron number per unit meter describes the power loss per unit meter. We plot the electron number per unit meter for the initial beam powers of 58 MW and 100 MW as two examples in Fig.9. One can see that over the first 200m the electron number is higher for 100 MW, which causes a bigger loss. After that the electron number per meter is close to the others and determined mostly by the oscillating behaviour of the filament. There are stronger oscillating behaviours for input powers of 100 and 345 MW than those for input powers of 58 and 185 MW (see Fig.7), which is associated with the larger variation of electron numbers in Fig.9. The small beam sizes at 1050m (for 100 MW) and 650m (for 345 MW) cause the large electron plasma densities. The high peaks in plasma density lead to such a strong plasma defocusing that cannot be compensated even by the slightly larger beam power in those filaments and ultimately causes the filament to diffract. When the oscillating behaviour is minimal, the case is out of this paper.

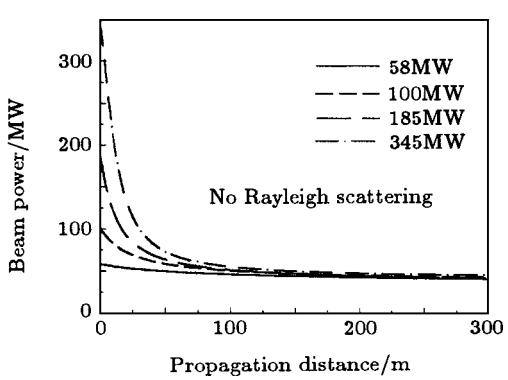


Fig.8. Beam powers versus distance for the initial powers of 58, 100, 185 and 345 MW without regarded to the Rayleigh scattering. The initial beam size is w_0=130μm.

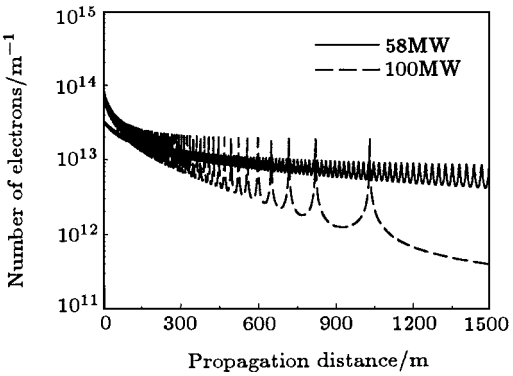


Fig.9. Number of electron per meter in filament versus distance for the initial powers of 58 MW (solid line) and 100 MW (dashed line) without regard to scattering loss. Note that it is different from electron density.

With regard to the Rayleigh scattering, all filaments propagate a length of 500m for the four initial powers. The beam size behaviours over the first 200m are very similar to those without regard to the scattering losses. The beam power is plotted in Fig.10. The power losses are dominated by photon ionization at either a higher or lower initial power over the first 200m. For the remaining distance, the loss is dominated by the Rayleigh scattering, which ultimately determines the propagation length. After about 500m, the beam power remains at the levels between 33 MW and 38 MW at which the beam cannot be trapped for all input powers. This is why all the filaments propagate the same length no matter what those input powers are.

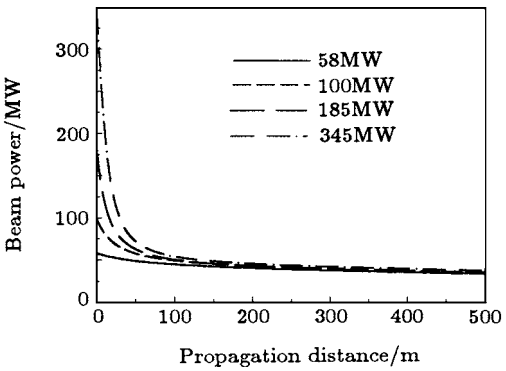


Fig.10. Beam powers versus distance for the initial powers of 58, 100, 185 and 345 MW with regard to the Rayleigh scattering. The initial beam size is w_0=130μm.

6. Conclusion

In general the filament propagation is characterized by a continuous beam size oscillation. This oscillation period and the beam size increase with propagation distance due to the loss of beam power caused by the 3-photon ionization and Rayleigh scattering. At the beginning of the filament propagation, the behaviours of the beam propagation are similar with and without regard to the Rayleigh scattering. Afterwards, the effect of Rayleigh scattering becomes more and more pronounced and determines the filament length. In the case of no Rayleigh scattering the filament length is determined by the oscillating behaviour of the beam, and the filament propagates the longest distance when the variation in beam size is minimal.

This work was done during visit to Diels research group at University of New Mexico as a visiting professor.

References

[1] Braun A, Korn G, Liu X *et al* 1995 *Opt. Lett.* **20** 73
[2] Nibbering E T J, Curley P F, Grillon G *et al* 1996 *Opt. Lett.* **21** 62
[3] Fontaine B, Vidal F, Jiang Z *et al* 1999 *Phys. Plasmas* **6** 1615
[4] Couairon A and Bergé L 2002 *Phys. Rev. Lett.* **88** 135003
[5] Couairon A, Tzortzakis S Bergé L *et al* 2002 *J. Opt. Soc. Am.* **B 19** 1117
[6] Couairon A 2003 *Phys. Rev.* A **68** 15801
[7] Schwarz J, Rambo P and Diels J C 2000 *Opt. Commun.* **180** 383
[8] Schwarz J and Diels J C 2001 *Phys. Rev.* A **65** 013806
[9] Tzortzakis S, Lamouroux B, Chiron A *et al* 2000 *Opt. Lett.* **25** 1270
[10] Tzortzakis S, Lamouroux B, Chiron A *et al* 2001 *Opt. Commun.* **197** 131
[11] Wen S C, Qian L J and Fan D Y 2003 *Acta Phys. Sin.* **52** 1640 (in Chinese)
[12] Duan Z L, Chen J P, Fang Z B *et al* 2004 *Acta Phys. Sin.* **53** 473 (in Chinese)
[13] Wen S C and Fan D Y 2001 *Chin. Phys.* **10** 1032
[14] Khan N, Marium N, Aris I *et al* 2002 *New Journal of Physics* **4** 61
[15] Zhao X M and Diels J C 1995 *IEEE J. Quantum Electronics* **31** 599
[16] Vidal F, Comtois D and Chien C Y 2000 *IEEE Trans. Plasma Sci.* **28** 418
[17] Wöste L, Wedekin C, Wille H *et al* 1997 *Laser Optoelektron* **29** 51
[18] Rairoux P, Schllinger H, Neirdeimer S *et al* 2000 *Appl. Phys.* B **71** 573
[19] Mlejnek M, Kolesik M and Moloney J V 1999 *Opt. Lett.* **83** 2938
[20] Raizer Y P 1966 *Soviet Physics USPEKH* **8** 650
[21] Ono S, Suzuki Y, Kozeki T *et al* 2002 *Appl. Opt.* **41** 7556